which was derived for flags of a similar weight per unit area to the present streamers but which were an order of magnitude larger in size and had a smaller length/width ratio. Equation (1) collapses the data sufficiently for most engineering purposes, as demonstrated by Fig. 4, in which $C_D\{s\rho g/w\}^{1/3}$ is plotted as a function of l/s. The difference between the two correlations suggests that neither is completely adequate to cope with a wide range of parameters which depart significantly from the original test conditions. This is because the fluid dynamics of a flapping streamer is so complicated and, in addition to the parameters used for the correlation, the drag probably also depends on the Reynolds number, the nondimensional frequency, the shape of the leading edge support, and the small amount of stiffness in the material.

Measurements were also made of the flapping frequency of the streamers for a range of velocities and length/width ratios. Briefly the results showed that the flapping frequency was approximately twice the calculated flapping frequency of a rigid lamina of a similar size, shape, and weight hinged at one end which is given by

$$f = \frac{1}{2\pi}\left\{\frac{3\rho U^2 2\pi g}{8[2(l/s) + 1]wl}\right\}^{1/2} \quad (3)$$

Reference

[1] Fairthorne, R. A., "Drag of Flags," Reports and Memoranda 1345, May 1930, Aeronautical Research Committee.

Velocity Distributions in the Wake of Spheres

C. Lahaye,* L. Jean,* and H. Doyle†
Defense Research Establishment Valcartier, Quebec, Canada

The use of sparks for the measurement of the velocity distribution in flowfields is based on the following principle: the passage of a spark is characterized by the ionization of a narrow filament of gas and by a strong emission of light. When the spark is made across a flowfield, the ionized filament is displaced at the velocity of the neutrals and successive sparks at intervals of less than 200 μsec retrace the displaced path of the first spark. Recording of the light emitted by the sparks on stereo-photographic plates yields a three-dimensional profile of the displacement which can be used together with the time interval between the sparks to derive the flowfield velocity distribution.

The application of the spark technique to the measurement of wake velocity behind projectiles in ballistic ranges has been described previously.[1] The repeatability and the reasonableness of the results have been shown by measurements made in the inviscid region of the wake of supersonic spheres.[2] In the determination of the mean velocity characteristics of the turbulent wake of hypersonic spheres, a large amount of data is required to achieve statistically meaningful results. The collection of the data has been facilitated by the development of equipment allowing the production of multiple spark sequences at different axial distances on the same firing. Figure 1 shows the stereo photographs of three sequences made at axial distances (from left to right) of 1000, 1500, and 2400 body diameters behind a 0.4-in.-diam sphere at velocity of 14,500 fps and ambient pressure of 100 torr. The time intervals between sparks were 75, 100, and 150 μsec, respectively. A sample size of about 10 radial profiles has been selected for the determination of the mean characteristics at each of the various fixed axial distances.

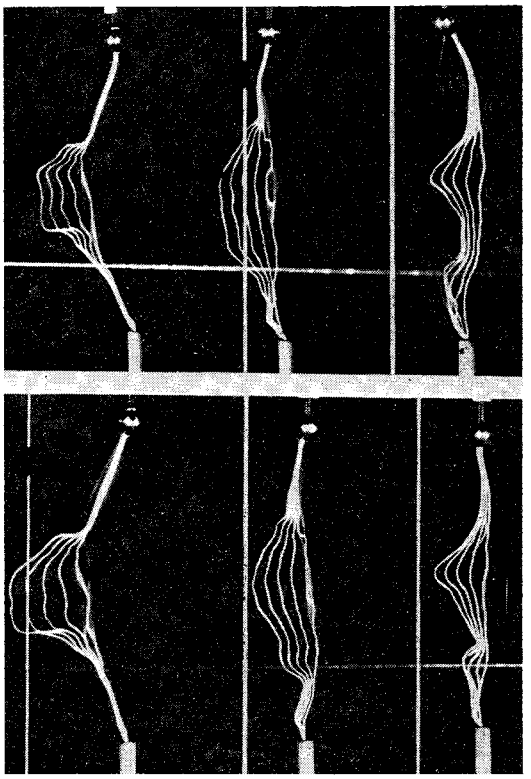

Fig. 1 Stereo photographs of three sequences of sparks at axial distances (from left to right) of 1000, 1500, and 2400 body diameters behind a 0.4-in. diam sphere (velocity: V_∞ = 14500 fps; ambient pressure: P_∞ = 100 torr); the spark intervals were 75, 100, and 150 μsec, respectively.

Figure 2 shows an example of a sample of 12 radial profiles of velocity collected at 300 body diameters behind 1-in.-diam spheres at 14,500 fps and 40 torr. The wake velocity V_w is normalized to the projectile velocity V_a and the radial dis-

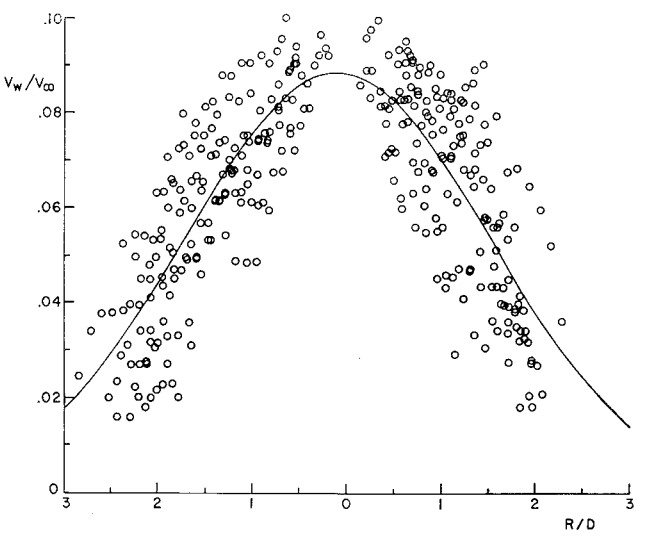

Fig. 2 Typical set of data from 12 measurements at 300 body diameters behind 1-in. diam spheres (V_∞ = 14500 fps; P_∞ = 40 torr); the wake axial velocity (V_w) is normalized to the sphere velocity (V_∞) and the radial distance (R) to the sphere diameter (D). Also shown is the slightly asymmetric gaussian curve fitted to the data.

Received March 27, 1969. Part of a joint DREV-ARPA Program under ARPA Order 133.

*Research Scientist, Aerophysics Division; also at Computing Devices of Canada.

† Technical Officer, Aerophysics Division.

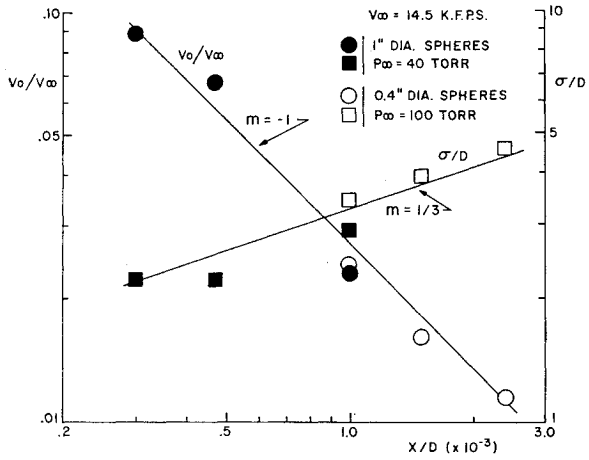

Fig. 3 Wake axis velocities (Vo/V_∞) and velocity profile widths (σ/D) determined from least mean squares fits of gaussian curves to sets of data measured at various axial distances (X/D). Full lines represent power laws with slopes of -1 and $\frac{1}{3}$ fitted to the wake axis velocity and the velocity profile width data, respectively.

tance R to the sphere diameter D. Study of a number of these samples measured at various axial distances has shown that the shape of the mean radial profiles is well approximated by gaussian curves. Accordingly, least mean square fits have been made on each of these samples of a modified gaussian expression of the form

$$V_w/V_a = (1 - R/aD)(V_o/V_a) \exp(-R^2/\sigma^2)$$

with R/D negative in the second quadrant in Fig. 2. In this expression, V_o/V_a is the normalized axis velocity and σ/D is a parameter related to the velocity radius. The factor $(1 - R/aD)$ has been introduced in the equation to account for the asymmetry of the radial profile due to ion mobility: the electric field applied to reilluminate the already formed ionized path induces a drift velocity of the ions. Calculations for conditions typical of the wake (P_a = 40 torr and temperature of 1000°K) indicate a displacement of the ions of 0.1 cm every time the spark path is reilluminated. To minimize this effect, only the axial displacement between the first two sparks of each sequence has been used to calculate the velocity. The curve in Fig. 2 is the asymmetric curve fitted to the data. The rms deviation of the data points with respect to the asymmetric mean curve is 0.0127 or 14.7% when normalized to the axis velocity. This value is reasonable if one takes account of the fact that it sums up contributions from turbulence intensity, goodness-of-fit, and accuracy of the experimental technique.

The results obtained from the least mean squares fits of the samples of data collected at various axial distances behind spheres at 14500 fps are given in Fig. 3. Two different size spheres have been used in order to avoid the troublesome interaction with the wake of the shock system arising from the reflection of the projectile bow and wake shocks by the cylindrical range tank.[3] Different pressures were used in order to have the same Reynolds' number (based on sphere diameter) of 0.4×10^6. Full symbols in Fig. 3 pertain to data measured behind 1-in.-diam spheres at 40 torr and open symbols to data obtained behind 0.4-in. spheres at 100 torr. Circles are used to indicate the wake axis velocity V_o/V_a and square to indicate the corresponding values of the profile width σ/D. Power laws with slopes of -1 and $\frac{1}{3}$ have been fitted to the wake axis velocity and the velocity profile width, respectively. It can be seen that the velocity decays roughly as $(X/D)^{-1}$ in the region covered by the data. The growth of the velocity core follows the well-established $\frac{1}{3}$ growth law of wakes. The radius of the wake observed by the schlieren technique[4] is equal to about 1.25 times the value of σ/D indicated in Fig. 3.

In Fig. 4, a comparison is made between sphere wake velocities measured in ballistic ranges by four different techniques. Full circles repeat the mean axis velocity data given in Fig. 3 at Mach 12.8 and a Reynolds number of 0.4×10^6. Half full circles represent axis velocities measured on individual profiles with the spark technique (M = 9.8–12.4, Re = 0.3×10^6). Full triangles are convection velocities of Heckman[5] obtained from the cross correlation of signals from axial arrays of electrostatic probes at M = 13.2 and Re = 0.55×10^6. These data collected at radial distances of 1.0–1.5 body diameters have been corrected for off-axis by assuming gaussian radial distributions of velocity and by using the fitted σ/D curve of Fig. 3. Full squares represent wake velocities measured by Herrmann, Slattery, and Clay[4] and determined from the cross correlation of density fluctuations on sequentially exposed schlieren photographs of the turbulent wake (M = 14.5, Re = 0.2×10^6). Open squares refer to mean wake velocities measured by Fox and Rungaldier[6] using hot wires calibrated in a heated jet and operated at temperature close to that of the wake to emphasize the velocity effect (M = 5.8 and Re = 1.6×10^6). The off-axis effect, more important at the smaller axial distances, has not been corrected in this case because the radial distance is not given. Convection velocity data obtained under the same conditions from the cross-correlation of signals from axial arrays of hot wires show lower velocity possibly due to technique[6,7] and have not been included. Finally, open circles represent the wake axis velocities obtained from radial profiles measured with the spark technique at M = 3.5 and Re = 0.1–0.5 $\times 10^6$ (Refs. 2 and 7). Full and half-full symbols have been used to represent measurements at high Mach number ($M > 10$) and open symbols for low Mach number ($M < 6$). Hypersonic data measured with the spark and electrostatic probe techniques show excellent agreement. Data obtained with the schlieren technique show appreciably lower velocity. This is due to the fact that the technique measures an average velocity across the wake and is possibly biased to measure the edge velocity because of the wake density distribution. The supersonic data show appreciably lower velocity in the intermediate wake region and coincide with hypersonic data past about 1000 body diameters. Asymptotic $-\frac{2}{3}$ power law decay is obtained from a distance between 1000 and 1500 body diameters for high Mach

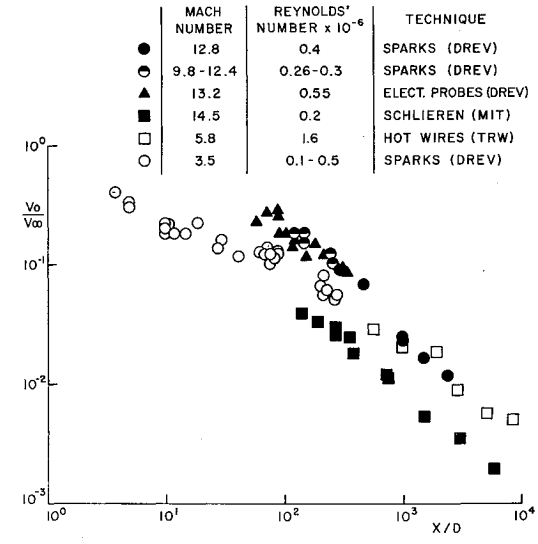

Fig. 4 Comparison of sphere wake velocities measured in ballistic ranges by four different experiments: sequential spark, electrostatic probe, hot wire, and sequential schlieren techniques.

number data and from about 500 body diameters for low Mach number data.

References

[1] Heckman, D., Tardif, L., and Lahaye, C., "Experimental Study of Turbulent Wakes in the CARDE Free-Flight Ranges," *Proceedings of the Symposium on Turbulence of Fluids and Plasmas*, Vol. XVIII, Polytechnic Press of the Polytechnic Institute of Brooklyn, N. Y., 1968.

[2] Lahaye, C., Leger, E. G., and Lemay, A., "Wake Velocity Measurements using a Sequence of Sparks," *AIAA Journal*, Vol. 5, No. 12, Dec. 1967, pp. 2274–2276.

[3] Heckman, D. et al., "A Shock Wave Attenuation Treatment for Ballistic Ranges," *AIAA Journal*, to be published.

[4] Herrmann, J., Slattery, R. E., and Clay, W. G., "Measured Properties of the Wakes of Hypersonic Cones," AIAA Paper 68-687, Los Angeles, Calif., 1968.

[5] Heckman, D., "Convection Velocity Measurements in Hypersonic Sphere Wakes." *AIAA Journal*, Vol. 6, No. 4, April 1968, pp. 750–752; also Heckman, D., private communication, 1969.

[6] Fox, J. and Rungaldier, H., "Anemometer Measurements of Velocity and Density in Projectile Wakes," AIAA Paper 68-701, Los Angeles, Calif., 1968.

[7] Ghosh, A. K. and Richard, C. "Probe Geometry Effect on Turbulent Plasma Diagnostics," Research Report 3.900.12, May 1968, R.C.A. Victor Company Ltd., Research Lab., Montreal.

[8] Lahaye, C., Leger, E. G., and Lemay, A., "Radial and Axial Velocity Profiles of Hypersonic and Supersonic Wakes Measured by the Sequential Spark Method," AGARD Conference Proceedings No. 19, Fluid Physics of Hypersonic Wakes Conference, May 1967.

Minimum-Time Attitude Maneuvers with Control Moment Gyroscopes

JACK KRANTON*

Bellcomm Inc., Washington, D. C.

A MANEUVER capability for large, Earth-orbiting spacecraft such as a space station may be required to acquire new inertial attitudes for particular experiments and to manage the angular momentum accumulated by a CMG (control moment gyroscopes) system.[1]

The solution to the maneuver problem with CMGs divides naturally into two parts, calculating the required control torque and commanding the CMG gimbal angle rates to produce that torque. Solutions to both problems are presented in this Note. These solutions can form the basis for implementation on flight hardware.

Rotation Angle and Rotation Axis

From Euler's rotation theorem,[2] it follows that any attitude maneuver can be expressed as a rotation through some angle (rotation angle) about some fixed axis (rotation axis). As in Ref. 3, $\mathbf{e}$ will denote the unit rotation vector and Φ the rotation angle. Both $\mathbf{e}$ and Φ are determined uniquely from the direction-cosine matrix between the coordinates that define the initial and final attitudes of the spacecraft.

During the maneuver $\mathbf{e}$ is fixed relative to inertial coordinates and spacecraft coordinates, but the rotation angle $\phi(t)$ decreases to zero; that is, $\phi(0) = \Phi$ and $\phi(T) = 0$ where T is the total maneuver time. It is convenient to change variables and define the angle λ such that $\lambda(t) = \Phi - \phi(t)$, then $\lambda(0) = 0$ and $\lambda(T) = \Phi \equiv \Lambda$.

Received March 2, 1970; revision received May 4, 1970.

* Supervisor, Rotational Dynamics and Attitude Control Group, Apollo Applications Division. Member AIAA.

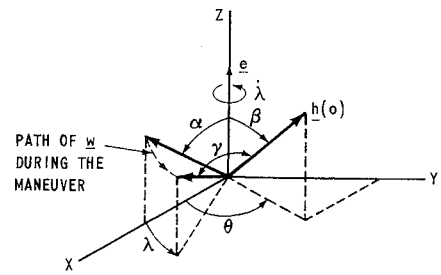

Fig. 1 Relationship between e, h (0), and w relative to inertial coordinates.

Control Torque for Minimum-Time Maneuver

The maneuver time will be minimum if at all times $\dot{\lambda}$ is maximized, subject to the constraint on the magnitude of the spin angular momentum vector $\mathbf{H}$ of the CMG system. For a system of N CMGs each with a spin angular momentum of h, $|\mathbf{H}| \leq Nh$.

To determine the maximum $\dot{\lambda}$, assume for the moment that the total angular momentum of the spacecraft and CMGs remains unchanged during the maneuver; that is, the effect of external torques is neglected during the maneuver. In vector-matrix notation, this can be stated as

$$\mathbf{H}(0) = \mathbf{H}(t) + I\boldsymbol{\omega} = \mathbf{H}(t) + \dot{\lambda}I\mathbf{e} \tag{1}$$

where $\mathbf{H}(0)$ and $\mathbf{H}(t)$ are the total CMG spin angular momenta at times 0 and t, I is the inertia matrix, and $\boldsymbol{\omega}(= \dot{\lambda}\mathbf{e})$ is the angular velocity of the spacecraft. Note that $\mathbf{H}(0)$ and $\mathbf{e}$ in Eq. (1) have a fixed orientation relative to inertial coordinates, but $\mathbf{H}(t)$ and $I\mathbf{e}$ do not. It is convenient now to introduce the following notation: $\mathbf{H} = |\mathbf{H}|\mathbf{h} \equiv H\mathbf{h}$, $I\mathbf{e} \equiv |I\mathbf{e}|\mathbf{w} \equiv W\mathbf{w}$ where $\mathbf{h}$ and $\mathbf{w}$ are unit vectors. With this notation, Eq. (1) can be rewritten as

$$H(t)\mathbf{h}(t) = -\dot{\lambda}W\mathbf{w} + H(0)\mathbf{h}(0) \tag{2}$$

By forming the self dot product on both sides of Eq. (2), one obtains a quadratic equation for $\dot{\lambda}$

$$H^2(t) = W^2\dot{\lambda}^2 - 2H(0)Wc\gamma\dot{\lambda} + H^2(0) \tag{3}$$

where $c\gamma = \mathbf{h}'(0)\mathbf{w}$ (sine and cosine are denoted by s and c). The maximum of $\dot{\lambda}$ is attained by choosing $H(t)$ to be the maximum Nh during the entire maneuver. Consequently, the maximum of $\dot{\lambda}$ is given by

$$\dot{\lambda} = \{H(0)c\gamma + [-H^2(0)s^2\gamma + (Nh)^2]^{1/2}\}/W \equiv f(\lambda) \tag{4}$$

The functional relation between $c\gamma$ and λ can be determined by noting (see Fig. 1) that the vectors $\mathbf{h}(0)$ and $\mathbf{e}$ are fixed, but $\mathbf{w}$ rotates about $\mathbf{e}$ with angular velocity $\dot{\lambda}$. From the geometry, it follows that

$$c\gamma = \mathbf{h}'(0)\mathbf{w} = c\alpha c\beta + s\alpha s\beta c(\lambda - \theta) \tag{5}$$

where α, β, and θ are constant angles determined at the start of the maneuver from†

$$c\alpha = \mathbf{w}'\mathbf{e},\ c\beta = \mathbf{h}'(0)\mathbf{e},\ (0 \leq \alpha < \pi/2,\ 0 \leq \beta \leq \pi) \tag{6a}$$

and

$$\theta = \theta^+ \operatorname{sgn}[\mathbf{e}'[\tilde{\mathbf{w}}\mathbf{h}(0)]]|_{\lambda=0} \tag{6b}$$

where

$$\theta^+ = \cos^{-1}[(\mathbf{h}'(0)\mathbf{w} - c\alpha c\beta)/s\alpha s\beta]|_{\lambda=0}\ (0 \leq \theta^+ \leq \pi) \tag{6c}$$

Certain properties of $f(\lambda)$ are evident. The extreme values of $f(\lambda)$ coincide with the extreme values of $c\gamma$, which

† The symbol $\sim$ over a vector indicates the cross product operation and the prime denotes transpose.